# ENERGY BALANCE IN MOBILE-BOUNDARY FLOWS: IMPLICATIONS FOR SEDIMENT TRANSPORT AND FLOW-BIOTA INTERACTIONS

PAPADOPOULOS K.[1]
NIKORA V.[1]
VOWINCKEL B.[2]
CAMERON S.[1]
FRÖHLICH J.[3]
STEWART M.[1]
BIGGS H.[1]
GIBBINS C.[4]

[1]*School of Engineering, the University of Aberdeen, King's College, Fraser Noble Building Aberdeen, AB24 3UE, United Kingdom*
[2]*Department of Mechanical Engineering, UC Santa Barbara, 2301 Engineering Building Santa Barbara, CA 93106, USA*
[3]*Institute of Fluid Mechanics, TU Dresden, George-Bähr-Straße 3c Dresden, D-01062, Germany*
[4]*School of Geosciences, the University of Aberdeen, King's College, Meston Building Aberdeen, AB24 3UE, United Kingdom*

The objective of this study is to identify and quantify the key physical mechanisms involved in the energy transfers in open-channel flows over mobile beds. This objective is achieved by assessing the relevant terms of the kinetic energy balances for mobile granular bed flows derived following the double-averaging methodology. The data underpinning this study are obtained from direct numerical simulations performed at the Dresden Technical University for open-channel flow over a granular bed with small relative submergence. It is anticipated that this investigation will assist in the analysis of experimental data sets and in the development of improved predictive open-channel flow models.

## 1 INTRODUCTION

Natural fluvial environments typically involve flow interactions with underlying mobile boundaries, such as river beds with active sediment transport or vegetation. The quantitative description of such complex systems can be appropriately achieved using the Double-Averaging Methodology (DAM) and the associated double-averaged hydrodynamic equations [1, 2]. This set of equations has been developed to establish the connection of the spatial and temporal variation of the boundary geometry with the dynamics of rough-bed open channel flows. The change of bed geometry typically induces roughness-scale effects in the near-bed velocity field. The conditions and behaviour of benthic communities (e.g., colonisation, nutrient availability and uptake, growth rate) strongly depend on the near-bed velocity field, as benthic organisms typically live within the roughness layer. Employing the double-averaged equations in the analysis of highly resolved data, such as those obtained by Direct Numerical Simulations (DNS), can assist in the identification of the key physical mechanisms of flow-boundary interactions. The present analysis is restrained to flows over granular beds; however, it can be equally applicable for flows over vegetation or mussel patches. In this paper, the estimates of the terms involved in the mean and form-induced kinetic energy balances are presented and analysed.

## 2 THEORETICAL FRAMEWORK AND COMPUTATIONAL SETUP

Following a general approach proposed in [3], the double-averaged second-order hydrodynamic equations can be derived as outlined below. The tensor notation is used throughout the paper where $i$ = 1, 2 and 3 define the longitudinal, transverse and vertical directions, respectively. The overbar and angle brackets are used to denote time and space averages, while deviations from mean values are indicated with primes and tildes, i.e., $\theta' = \theta - \overline{\theta}$ and $\tilde{\theta} = \theta - \langle\theta\rangle$. The equation obtained for the balance of the 'double-averaged' kinetic energy (DKE) within the Eulerian framework is given below:

$$\underbrace{\frac{1}{2}\frac{\partial \phi_{VT}\langle \overline{u}_i\rangle^2}{\partial t}}_{\text{(1) rate of MKE}}+\underbrace{\frac{\partial \phi_{Vm}\langle \phi_T\tilde{\overline{u}}_i\langle \overline{u}_i\rangle\rangle}{\partial t}}_{\text{(2) rate of mobility contribution}}+\underbrace{\frac{1}{2}\frac{\partial \langle \overline{u}_i\rangle^2\phi_{VT}\langle \overline{u}_j\rangle}{\partial x_j}}_{\text{(3) convection of MKE}}+\underbrace{\frac{\partial \phi_{Vm}\langle \phi_T\tilde{\overline{u}}_i\langle \overline{u}_i\rangle\rangle\langle \overline{u}_j\rangle}{\partial x_j}}_{\text{(4) convection of mobility contribution}}+\underbrace{\frac{1}{2}\frac{\partial \langle \overline{u}_i\rangle^2\phi_{Vm}\langle \phi_T\tilde{\overline{u}}_j\rangle}{\partial x_j}}_{\text{(5) convection of MKE}}$$

$$\underbrace{-\phi_{Vm}\langle \phi_T\tilde{\overline{u}}_i\rangle\frac{\partial \langle \overline{u}_i\rangle}{\partial t}}_{\text{(6)}}=\underbrace{\phi_{VT}\langle \overline{u}_i\rangle g_i}_{\text{(7) gravitational input}}\underbrace{-\frac{1}{\rho}\frac{\partial \phi_{Vm}\langle \phi_T\overline{p}\rangle\langle \overline{u}_i\rangle}{\partial x_i}}_{\text{(8) pressure transport}}\underbrace{-\frac{\partial \phi_{Vm}\langle \phi_T\overline{u_i'u_j'}\rangle\langle \overline{u}_i\rangle}{\partial x_j}}_{\text{(9) turbulent transport}}\underbrace{-\frac{\partial \phi_{Vm}\langle \phi_T\tilde{\overline{u}}_i\tilde{\overline{u}}_j\rangle\langle \overline{u}_i\rangle}{\partial x_j}}_{\text{(10) form-induced transport}}$$

$$\underbrace{+\frac{1}{\rho}\frac{\partial \phi_{Vm}\langle \phi_T\overline{\tau}_{ij}\rangle\langle \overline{u}_i\rangle}{\partial x_j}}_{\text{(11) viscous transport}}+\underbrace{\frac{\phi_{Vm}\langle \phi_T\overline{p}\rangle}{\rho}\frac{\partial \langle \overline{u}_i\rangle}{\partial x_i}}_{\text{(12) pressure work against mean strain rate}}\underbrace{-\frac{\phi_{Vm}\langle \phi_T\overline{\tau}_{ij}\rangle}{\rho}\frac{\partial \langle \overline{u}_i\rangle}{\partial x_j}}_{\text{(13) conversion to heat}}+\underbrace{\phi_{Vm}\langle \phi_T\overline{u_i'u_j'}\rangle\frac{\partial \langle \overline{u}_i\rangle}{\partial x_j}}_{\text{(14) conversion to TKE}}+\underbrace{\phi_{Vm}\langle \phi_T\tilde{\overline{u}}_i\tilde{\overline{u}}_j\rangle\frac{\partial \langle \overline{u}_i\rangle}{\partial x_j}}_{\text{(15) exchange rate with FKE}}$$

$$\underbrace{+\phi_{Vm}\langle \phi_T\tilde{\overline{u}}_i\rangle\langle \overline{u}_j\rangle\frac{\partial \langle \overline{u}_i\rangle}{\partial x_j}}_{\text{(16) exchange rate with FKE}}+\underbrace{\frac{1}{\rho V_o}\langle \overline{u}_i\rangle\overline{\int_{S_{\text{int}}}\left(p\delta_{ij}-\tau_{ij}\right)n_j dS}^{\,s}}_{\text{(17) exchange with the boundary}}, \tag{1}$$

where $u_i$ is the $i^{\text{th}}$ velocity component, $g_i$ is gravity acceleration, $\rho$ is fluid density (considered constant), $\tau_{ij}$ is viscous stress, $n_i$ is the unit vector normal to interfacial surface $S_{\text{int}}$ and directed into the fluid, $\phi_{Vm}$ and $\phi_T$ are the space and time porosity functions [1], respectively. The balance of the form-induced kinetic energy (FKE) is obtained as:

$$\underbrace{\frac{\partial \frac{1}{2}\phi_{Vm}\langle \phi_T\tilde{\overline{u}}_i\tilde{\overline{u}}_i\rangle}{\partial t}}_{\text{(1) rate of FKE}}+\underbrace{\frac{\partial \frac{1}{2}\phi_{Vm}\langle \phi_T\tilde{\overline{u}}_i\tilde{\overline{u}}_i\rangle\langle \overline{u}_j\rangle}{\partial x_j}}_{\text{(2) convection of FKE}}+\underbrace{\phi_{Vm}\langle \phi_T\tilde{\overline{u}}_i\rangle\frac{\partial \langle \overline{u}_i\rangle}{\partial t}}_{\text{(3)}}=\underbrace{\phi_{Vm}\langle \phi_T\tilde{\overline{u}}_i\rangle g_i}_{\text{(4) gravitational input}}$$

$$\underbrace{-\phi_{Vm}\langle \phi_T\tilde{\overline{u}}_i\tilde{\overline{u}}_j\rangle\frac{\partial \langle \overline{u}_i\rangle}{\partial x_j}}_{\text{(5) exchange rate with DKE}}\underbrace{-\phi_{Vm}\langle \phi_T\tilde{\overline{u}}_i\rangle\langle \overline{u}_j\rangle\frac{\partial \langle \overline{u}_i\rangle}{\partial x_j}}_{\text{(6) exchange rate with DKE}}\underbrace{-\frac{1}{\rho}\frac{\partial \phi_{Vm}\langle \phi_T\tilde{\overline{u}}_i\overline{p}\rangle}{\partial x_i}}_{\text{(7) pressure transport}}\underbrace{-\frac{\partial \phi_{Vm}\langle \phi_T\tilde{\overline{u}}_i\overline{u_i'u_j'}\rangle}{\partial x_j}}_{\text{(8) turbulent transport}}\underbrace{-\frac{\partial \frac{1}{2}\phi_{Vm}\langle \phi_T\tilde{\overline{u}}_i\tilde{\overline{u}}_i\tilde{\overline{u}}_j\rangle}{\partial x_j}}_{\text{(9) form-induced transport}}$$

$$\underbrace{+\frac{1}{\rho}\frac{\partial \phi_{Vm}\langle \phi_T\overline{\tau}_{ij}\tilde{\overline{u}}_i\rangle}{\partial x_j}}_{\text{(10) viscous transport}}+\underbrace{\frac{\phi_{Vm}}{\rho}\left\langle \phi_T\overline{p}\frac{\partial \tilde{\overline{u}}_i}{\partial x_i}\right\rangle}_{\text{(11) pressure-strain rate correlation}}\underbrace{-\frac{\phi_{Vm}}{\rho}\left\langle \phi_T\overline{\tau}_{ij}\frac{\partial \tilde{\overline{u}}_i}{\partial x_j}\right\rangle}_{\text{(12) conversion to heat}}+\underbrace{\phi_{Vm}\left\langle \phi_T\overline{u_i'u_j'}\frac{\partial \tilde{\overline{u}}_i}{\partial x_j}\right\rangle}_{\text{(13) exchange rate with TKE}}+\underbrace{\frac{1}{\rho V_o}\overline{\int_{S_{\text{int}}}\left(\tilde{\overline{u}}_i p\delta_{ij}-\tilde{\overline{u}}_i\tau_{ij}\right)n_j dS}^{\,s}}_{\text{(14) exchange with the boundary}}. \tag{2}$$

The terms of Eqs (1) and (2) are estimated using the DNS data reported in [4] for turbulent open-channel flow over a mobile granular bed. The key simulation parameters are summarized in Table 1. The bed is composed of a subsurface layer of fixed particles and an overlying (i.e. surface) layer of mobile particles. The bulk Reynolds number is $\text{Re}_b = 2700$. The ratio of the simulation Shields number to the critical Shields number is $\Theta/\Theta_{\text{crit}} = 0.7$, which is indicative of near-critical bed conditions.

Table 1. Key parameters of the simulation scenario [4] ($H$ denotes the flow depth, $D$ is the particle diameter, $\Delta z$ is the cell size and $L_x$, $L_y$, $L_z$ denote the domain's extents in the $x$, $y$ and $z$ directions).

| $Re_b$ | $D^+$ | $H/D$ | $D/\Delta z$ | $\Theta/\Theta_{\text{crit}}$ | $L_x$ | $L_y$ | $L_z$ |
|---|---|---|---|---|---|---|---|
| 2700 | 19.2 | 9 | 22.2 | 0.7 | 12$H$ | 6$H$ | $H + D$ |

## 3 RESULTS

Following an analysis that involves checking the convergence of statistical estimates for first and second order moments (e.g. $\overline{u}$, $\langle \overline{u}\rangle$, $\overline{u'u'}$, $\langle \overline{u'u'}\rangle$ and $\phi_{VT}$) and the appropriate resolution of the averaged hydrodynamic variables, the averaging domains were defined. The total simulation time (after steady-state conditions are established) is selected as the averaging time. The dimensions of the averaging volume were selected as $(L_x, L_y, \Delta z)$. As a result, the averaged variables obtained are a function of the vertical coordinate only. Thus, the terms involving derivatives with respect to $t$, $x$ and $y$ coordinates are equal to zero. For the estimation of derivatives with respect to $z$, a second-order accurate, finite central difference scheme is used. Terms 17 and 14 of Eqs (1) and (2), respectively, are not estimated because the integrals for the pressure and viscous forces cannot be calculated using the immersed boundary method applied in the numerical simulations [4].

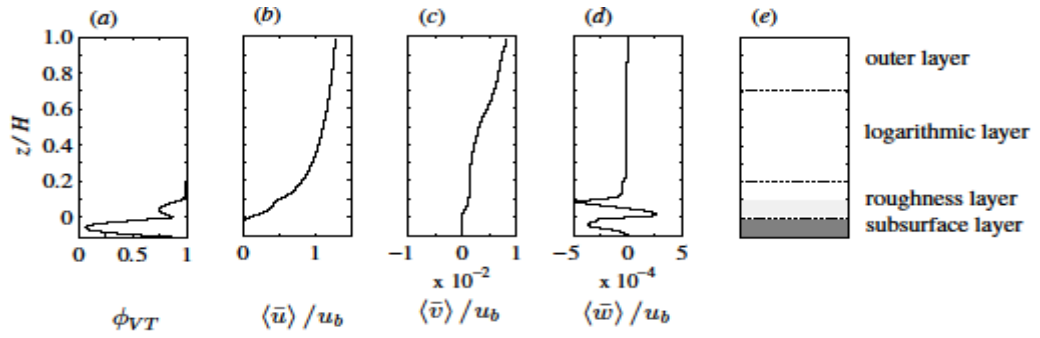


Figure 1. Vertical distributions of the space-time porosity, defined in [1], the double-averaged velocity components, normalized by the bulk velocity and a sketch with the flow subdivision into layers.

The distributions of the space-time porosity $\phi_{VT}$ and three components of the double-averaged velocity vector presented in Figure 1 highlight some near bed features related to particle movements. The vertical distributions of the terms describing convection, transport, and energy conversion ('production' or 'dissipation') are shown in Figures 2 and 3, allowing estimation of their significance. The distances/lengths and velocities involved in the terms of Eqs (1) and (2) are normalized by the flow depth $H$ and the bulk flow velocity $u_b$ (i.e., depth-averaged value of $\langle\bar{u}\rangle$). The terms involved in the kinetic energy balances and shown in Figures 2 and 3 are normalized by $gu_b$, which is considered as indicative of the kinetic energy input into the system.

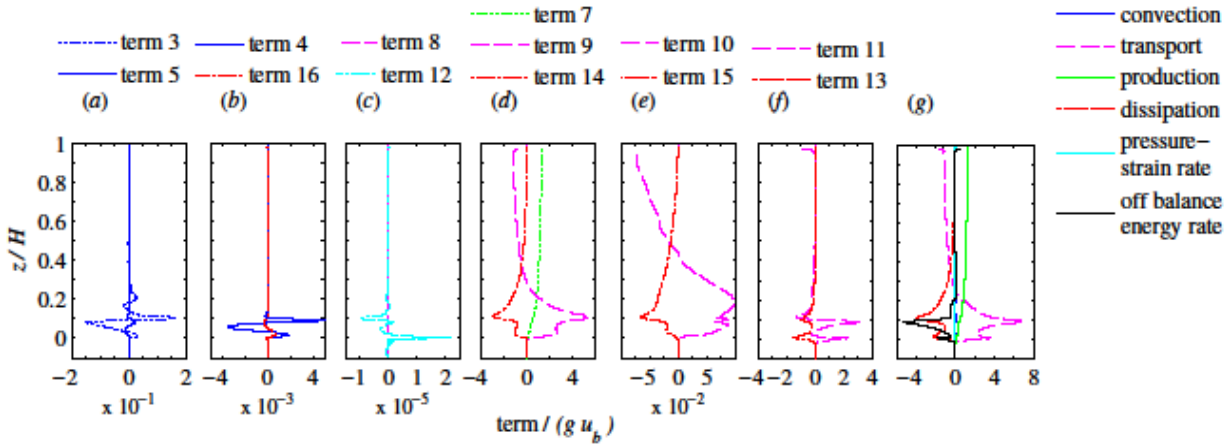


Figure 2. Vertical distributions of the terms contributing to the 'double-averaged' kinetic energy budget (*a-f*) and the budget summary (*g*).

A summary of the mechanisms involved in the kinetic energy balances, described by Eqs (1) and (2), is given in Figures 2*g* and 3*f*. The spatial distribution of the porosity (Figure 1*a*) is indicative of bed morphology. The lowest values are observed below z/*H* = 0, where the fixed particles are placed. The additional layer of mobile particles is represented by $0.7 < \phi_{VT} < 1$ for $0 < z / H < 0.1$. As expected, the longitudinal velocity component is much more significant than the transverse and vertical components, which are close to zero. The effect of the particle layers on the flow is evident in Figures 2 and 3, as the parameter distribution peaks are located at *z*/*H* = 0.1; i.e., at the interface between the particle-dominated and the particle-clear flow regions. It seems that the terms involving the Reynolds stress (turbulent transport, turbulent work rate against strain rates) dominate the energy transport and conversion in both balances. Terms containing the correlation of $\phi_T$ and $\tilde{\tilde{u}}_i$ may not be insignificant as initially anticipated (compare distributions of terms 3 and 5 in the DKE balance; Figure 2*a*). An interesting feature is the behavior of term 13 in the FKE balance. This term represents the exchange of the energy between FKE and turbulent kinetic energy (TKE) balances. Below the level *z*/*H* = 0.1, FKE is converted into TKE, while just above it the opposite conversion happens. However, the data on the TKE balance are needed before any firm conclusions can be drawn. In Eq. (1), term 4 appears to be negligible compared to terms 3 and 5. From the transport-associated terms, the 8th and 10th terms are insignificant compared to terms 9 and 11. By comparing the energy deducting terms one may note that terms 13 and 14 are much larger than terms 15 and 16 (Figures 2*a-f*).

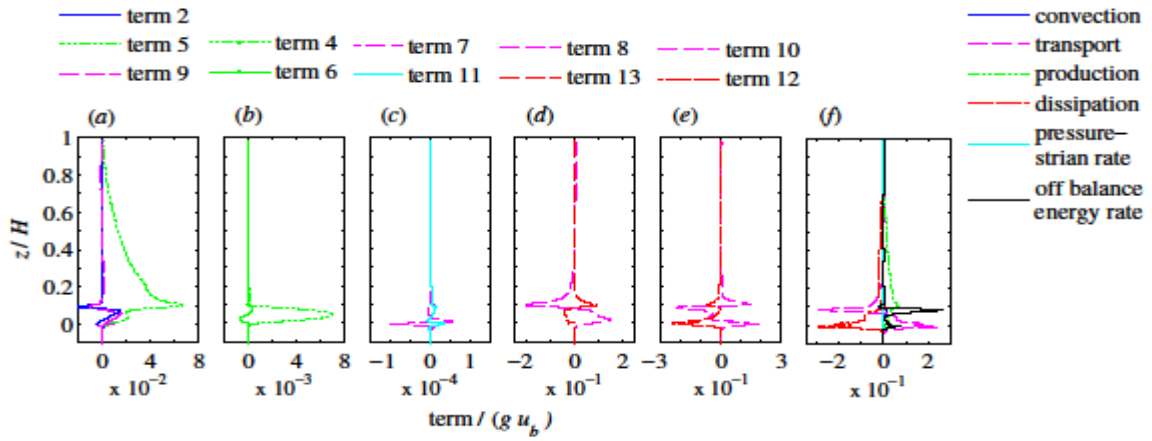


Figure 3. Vertical distributions of the terms contributing to the form-induced kinetic energy budget (*a*-*e*) and the budget summary.

Among the transport terms of Eq. (2), terms 7, 9 are negligible compared to the 8th and 9th terms. Terms 4, 5 and 13 are all significant terms of the energy conversion (Figures 3*a*-*e*). The off-balance energy rates were found as the balance residuals, by deducting the RHS terms from the LHS, for each equation. Given that the last terms of Eqs (1) and (2) (i.e., interfacial terms) are the only terms that are not estimated, the off-balance energy rates could be indicative of the interfacial kinetic energy exchange. Following this point, the data show that the substantial amount of mean kinetic energy is driven to the particle motion. On the contrary, form-induced flow receives kinetic energy from the boundary to convert it mainly into turbulence and heat.

## 4 CONCLUSIONS

The present paper employs the DAM-based energy balance equations in the analysis of a data set obtained by DNS, with the focus on the balance of specific kinetic energy components. An investigation of the FKE balance is reported for the case of a mobile-boundary flow. It is anticipated that this analysis, complemented with the investigation of the turbulent kinetic energy balance and extended for smaller averaging volumes, will assist in the study of complex flows such as those over mobile granular beds.

## ACKNOWLEDGMENTS

This study is a part of the research project “Hydrodynamic Transport in Ecologically Critical Heterogeneous interfaces” (HYTECH), the support of which, under the European Union's Seventh Framework Programme (Marie Curie FP7-PEOPLE-2012-ITN, European Commission grant agreement 316546), is gratefully acknowledged. It was also partially supported by the UK EPSRC grant EP/K041169/1, Bed friction in rough-bed free-surface flows: a theoretical framework, roughness regimes, and quantification, and partly funded by the German Research Foundation (DFG) via the project FR1593/5-2. The authors are grateful to two anonymous reviewers for the useful comments and suggestions.

## REFERENCES

[1] Nikora V., Ballio F., Coleman S. and Pokrajac D., “Spatially averaged flows over mobile rough beds: Definitions, averaging theorems and conservation equations”, *Journal of Hydraulic Engineering*, Vol. 139, No. 8, (2013), pp 803-811.

[2] Papadopoulos K., Nikora V., Cameron S., Stewart M., Biggs H. and Gibbins C., “Second-order hydrodynamic equations for flow over mobile boundaries and their applications for solving environmental problems”, *Proceedings of the 36th IAHR World Congress*, the Hague, the Netherlands, (2015).

[3] Keller L. and Friedmann A., “Differentialgleichung für die turbulente Bewegung einer kompressiblen Flüssigkeit”, *In* C. Biezeno, & J. Burgers (Ed.), *Proceedings of 1st International Congress of Applied Mechanics*, Delft: J. Waltman Jr. (1924), pp 395–405.

[4] Vowinckel B. and Fröhlich J., “Simulation of bed load transport in turbulent open channel flow”, *Proceedings in Applied Mathematics and Mechanics*, Vol. 12, No. 1, (2012), pp 505 - 506.